Pac-man motility of kinetochores unleashed by laser microsurgery

James R. LaFountain, Jr.[a], Christopher S. Cohan[b], and Rudolf Oldenbourg[c,d]
[a]Department of Biological Sciences, University at Buffalo, Buffalo, NY 14260; [b]Department of Pathology and Anatomy, University at Buffalo, Buffalo, NY 14214; [c]Marine Biological Laboratory, Cellular Dynamics Program, Woods Hole, MA 02543; [d]Physics Department, Brown University, Providence, RI 02912

ABSTRACT We report on experiments directly in living cells that reveal the regulation of kinetochore function by tension. X and Y sex chromosomes in crane fly (*Nephrotoma suturalis*) spermatocytes exhibit an atypical segregation mechanism in which each univalent maintains K-fibers to both poles. During anaphase, each maintains a leading fiber (which shortens) to one pole and a trailing fiber (which elongates) to the other. We used this intriguing behavior to study the motile states that X-Y kinetochores are able to support during anaphase. We used a laser microbeam to either sever a univalent along the plane of sister chromatid cohesion or knock out one of a univalent's two kinetochores to release one or both from the resistive influence of its sister's K-fiber. Released kinetochores with attached chromosome arms moved poleward at rates at least two times faster than normal. Furthermore, fluorescent speckle microscopy revealed that detached kinetochores converted their functional state from reverse pac-man to pac-man motility as a consequence of their release from mechanical tension. We conclude that kinetochores can exhibit pac-man motility, even though their normal behavior is dominated by traction fiber mechanics. Unleashing of kinetochore motility through loss of resistive force is further evidence for the emerging model that kinetochores are subject to tension-sensitive regulation.

INTRODUCTION

Tension is an essential component of the mechanism that facilitates segregation of chromosomes during either mitosis or meiosis. After the biorientation of chromosomes to opposite spindle poles by kinetochore fibers, tension results from pulling forces toward the poles and is a stabilizing factor that maintains proper orientation before anaphase onset and segregation (for a review, see Nicklas, 1997). Tension-related mechanisms are particularly evident during meiosis in spermatocytes from such insects as grasshoppers (Nicklas and Koch, 1969; Nicklas and Ward, 1994) and crane flies (Begg and Ellis, 1979a,b). We used the latter in the present work to address questions concerning the influence of tension on kinetochore function.

We have been engaged in experiments that ask what happens when tension on kinetochores is rapidly relieved. The rationale behind such an approach is to test a current model for spindle mechanics proposed by Maddox *et al.* (2003), who ascribe significance to tension in controlling the functional state(s) of kinetochores. The model is based on an important study performed on anaphase kinetochores in *Xenopus* oocyte extract spindles, showing kinetochores to switch from persistent depolymerization (pac-man) to persistent polymerization (reverse pac-man) and back again during the course of their poleward movement. Mechanical tension was proposed to be the critical factor in regulating those states; in the model by Maddox *et al.* (2003), kinetochores engaged in depolymerization are under low tension, whereas a switch to polymerization occurs in kinetochores that are under greater (or high) tension. The latter state is similar to metaphase, when kinetochores are assumed to be under high tension as a consequence of the poleward pulling action of the flux machine (Waters *et al.*, 1996). That would lead to functioning in a polymerization state, manifesting a "slip clutch" mechanism that would prevent detachment of microtubule plus ends under high tension (also see Mitchison, 2005).
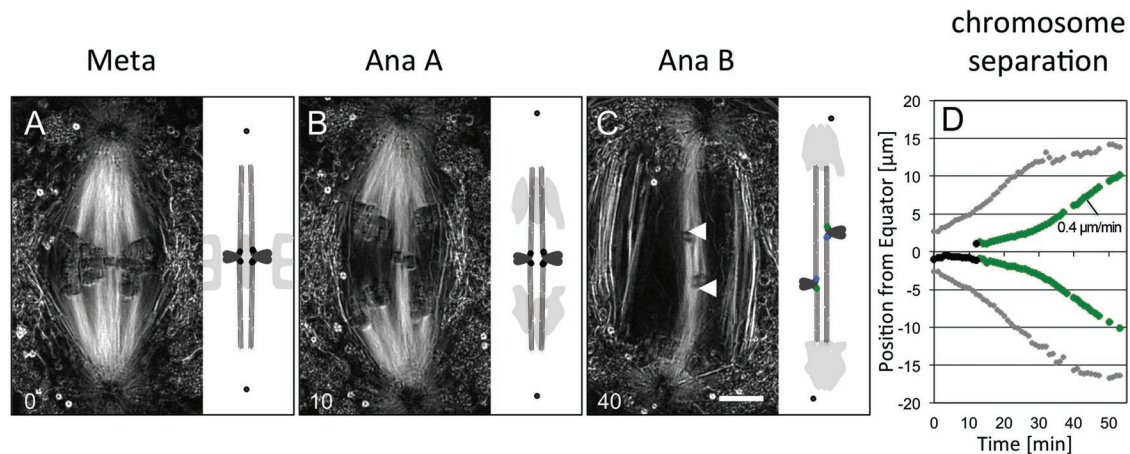
FIGURE 1: (A-C) LC-PolScope images and schematic drawings of X and Y sex univalents that exhibit amphitelic orientation at metaphase (A), anaphase A (B), and anaphase B (C) of meiosis I in crane fly spermatocytes. (B) Schematic: the univalents remain at the spindle equator as anaphase laggards, while disjoined autosomes (shaded chromosomes) undergo anaphase A segregation. (C) Anaphase B: spindle elongation increases the distance between segregated autosomes, and X and Y start segregating to opposite poles. Note that this cell has been flattened intentionally in order to image all of the chromosomes and their K-fibers in one focal plane, whereas the cells in Supplemental Movie S1 are not flattened. Hence anaphase B spindle elongation evident in nonflattened cells occurs in flattened cells as bending of the spindle, as is evident in C by centrosomes moving sideways instead of directly away from each other. Each laggard develops a leading kinetochore (arrowheads in C; green kinetochore in C, schematic) and a leading K-fiber, and a trailing kinetochore (blue kinetochore in C, schematic) and its trailing K-fiber. Trailing fibers elongate. Leading fibers shorten. (D) In the graph, autosomal anaphase A (gray dots) precedes X-Y segregation, during which the distances between leading kinetochores (green dots) of X and Y are plotted as a function of time based on data acquired from the cell included in Supplemental Movie S1. A–C, lower left: time in minutes; scale bar in C, 5 μm.

In a recent study on crane fly spermatocytes, we used a laser microbeam to sever kinetochores from chromosomes in order to rapidly relieve tension and release the detached kinetochore to move toward the pole to which it remained connected by its kinetochore fiber. In these meiotic cells, it is well documented that during the initial stages of anaphase, kinetochores retain the polymerization state that was evident at metaphase (LaFountain *et al.*, 2004; reviewed by Rogers *et al.*, 2005). Such retention is believed to be a consequence of tension imposed by elastic tethers that connect partner homologues during their segregation (LaFountain *et al.*, 2002). Anaphase by reverse pac-man is achieved because the rate of subunit addition to microtubule plus ends at kinetochores is slower than the rate of subunit loss from minus ends at the pole (LaFountain *et al.*, 2004). The bundle of kinetochore microtubules behaves as a fluxing traction fiber, with shortening occurring only at their minus (poleward) ends and with minus end–directed forces being generated at some location(s) other than the kinetochore, for example, along the length of the fiber, at the poles, or both.

In these experiments, through combining fluorescent speckle microscopy with kinetochore detachment operations, we found that released anaphase kinetochores of autosomes switched states from reverse pac-man to park, the latter being a functional state in which a kinetochore is anchored to the plus ends of its kinetochore microtubules. In park, there is neither gain nor loss of subunits at plus ends (LaFountain *et al.*, 2011).

Now we report on results from similar experiments, but instead of kinetochores of autosomes, we released the kinetochores of univalent sex chromosomes in crane fly spermatocytes. The results were similar and yet surprising and subtly different from the autosome story. Instead of switching to park, released kinetochores of sex chromosomes (normally engaged in reverse pac-man) switched to pac-man motility, in accord with the Maddox *et al.* (2003) model.

In the present study, we focused on kinetochores of X-Y univalents in crane fly spermatocytes during anaphase A and anaphase B of meiosis I. Kinetochores of X and Y are especially suited for these experiments because X and Y both maintain kinetochore fibers to both poles during their segregation. During X-Y segregation, the leading fiber of each shortens, and each trailing fiber elongates. Trailing fibers have long been viewed as imparting tension that resists poleward movement (Fuge, 1972, 1985) and likely accounts for the initially slow rate of segregation of X from Y. We used a laser microbeam to sever this normal bipolar connection of X-Y kinetochores and subsequently monitored the effect of such disconnections on the motility and function of the kinetochores and their kinetochore fibers that remained intact after the operation.

RESULTS

In the transition from metaphase (Figure 1A) to anaphase A (Figure 1B) of meiosis I, univalent X and Y both have connections to both spindle poles (amphitelic orientation), and they remain at the spindle equator as laggards during anaphase A (Figure 1B). Then, as anaphase B begins, X and Y segregate from each other, each developing a leading kinetochore (green dot in Figure 1C, schematic) and trailing kinetochore (blue dot in Figure 1C, schematic), while their respective kinetochore fibers (K-fibers) remain connected to the poles. As segregation proceeds, fibers connected to leading kinetochores (leading K-fibers) shorten and trailing K-fibers elongate (Figure 1C). Kinetochore fibers are imaged with striking clarity in living cells with liquid crystal polarized light microscopy (LC-PolScope), as is evident in Figure 1, A–C, and Supplemental Movie S1.

Two facets of this unusual sex chromosome segregation are most relevant to the present study: 1) the rate of chromosome movement during X-Y segregation and 2) the rate of microtubule flux within sex chromosome K-fibers. To measure segregation rates,

	Anaphase A		Anaphase B	
	Maximal rate	Steady-state rate	Maximal rate	Steady-state rate
X-Y segregation in control cells (Figure 1D)			0.5 ± 0.1 (range, 0.3–0.6, n = 18)	
After bisection of X or Y (red dots in Figures 3D, 4D)	1.4 ± 0.2 (range, 1.1–1.7, n = 11)	0.5 (n = 2)	1.4 ± 0.4 (range, 1.1–1.9, n = 3)	
After K ablation (red dots in Figures 3H, 4H)	1.3 ± 0.3 (range, 0.9–1.7, n = 16)	0.7 ± 0.2 (range, 0.5–1.0, n = 8)	1.3 ± 0.3 (range, 0.9–1.7, n = 7)	0.6 ± 0.1 (range, 0.5–0.7, n = 4)
Speckle velocities from kymographs[a]		0.8 ± 0.2 (range, 0.4–1.4, n = 15) [78]		
Speckles in leading fibers[a]				0.4 ± 0.1 (range, 0.2–0.6, n = 7) [18]
Speckles in trailing fibers[a]				0.4 ± 0.1 (range, 0.2–0.7, n = 7) [37]

n, number of cells; number in square brackets, number of speckle tracks.
[a]Anaphase B averages for leading and trailing fibers are not significantly different (t test, p = 0.29), whereas differences between anaphase A average and anaphase B averages are significant (p < 0.001).

TABLE 1: Summary of chromosome velocities away from the equator and rates of speckle flow in crane fly spermatocytes undergoing meiosis I.

we did frame-by-frame analysis of time-lapse movies. To measure flux rates, we applied fluorescent speckle microscopy to spermatocytes injected with rhodamine (Rh)-tubulin and then analyzed movement of fluorescent speckles in kymographs made from time-lapse recordings of speckle flow.

X-Y movement reaches a maximal velocity when separation is 12–15 μm

From movies of control cells undergoing anaphase, we measured the distance separating X and Y for every frame, and from plots of those measurements we determined the maximal speed of separation, as shown in the graph in Figure 1D. To standardize such data to a common reference, we chose to use the equator as the reference point for reporting all of our data, including results obtained after the laser microbeam operations that we describe in the following sections.

Using the plot in Figure 1D as a representative example, we note the slowly accelerating rate of segregation, which reaches a maximum of 0.4 μm/min away from the equator at a separation distance of ~14 μm.

On the basis of data compiled from 18 control cells presented in Table 1, we found the average maximal rate of segregation away from the equator to be 0.5 ± 0.1 μm/min, and in all cases, this was only after X and Y had been separated by a significant distance of 12–15 μm.

Fluorescent speckles move faster than kinetochores in early anaphase B

To establish a baseline for the movement of X-Y kinetochores in relation to microtubule flux in their K-fibers, we performed fluorescent speckle microscopy of cells both before (Figure 2, A and B) and during (Figure 2, D and E) X-Y segregation.

When fluorescent speckle microscopy was done on cells already in an anaphase B stage such as in Figure 1C, their kinetochores exhibited polymerization function. Right after injection of Rh-tubulin at that stage, flux was evident in both leading and trailing K-fibers, and speckles were observed emanating from both leading and trailing kinetochores. From kymograph analysis of movies (such as Supplemental Movie S2, top and bottom, and Figure 2, D–F), the average flux rate was 0.4 μm/min (Table 1), whereas chromosome velocities

in the same cells did not exceed 0.3 μm/min away from the equator. Furthermore, flux rates in leading and trailing K-fibers of a given sex chromosome were similar (Table 1), revealing a significant difference in the polymerization rates of leading and trailing kinetochores, as will be discussed.

With regard to measuring flux in K-fibers during the course of X-Y segregation, there was a limitation in the portion of segregation that was amenable to this approach. In early stages of anaphase B, such as in Figures 1C and 2, D and E, we could distinguish fluorescent speckles in both leading and trailing fibers. Such speckles were also analyzed in the presented kymographs. However, the inherent nature of this segregation mechanism causes K-fibers of X and Y to become very closely aligned during later stages. This makes it impossible to distinguish the leading and trailing fibers of one from those of the other, and, thus, analysis of flux cannot be performed accurately at stages later than that diagrammed in Figure 1C (schematic). The point at which distinctions cannot be made is ~8–10 μm of separation, beyond which speckle analysis becomes impractical. Hence, experiments reported here were done only on cells in the early stages of anaphase B, before the time when such close apposition of K-fibers occurred.

Fluorescent speckle microscopy of cells in anaphase A (Figure 2, A and B)—before X-Y segregation starts—revealed fast microtubule flux within X-Y K-fibers, faster, in fact, than that observed during early anaphase B. This is evident in Supplemental Movie S2, top and bottom, as well as in the representative kymograph in Figure 2C, which was made from Supplemental Movie S2, top. Data from further analysis of kymographs presented in Table 1 shows an average flux rate of 0.8 μm/min away from the equator. Thus it is clear from speckle movies that X-Y kinetochores positioned motionless at the equator in anaphase A were also in a polymerization state, adding fluorescent subunits that then move poleward via microtubule flux. Moreover, the faster average flux rate for anaphase A (Table 1) indicates a slowdown in the flux mechanism in the transition from anaphase A to anaphase B.

Kinetochores released from bipolar connections exhibit rapid poleward movement

Having established that sex kinetochores were functioning in a polymerization state, we performed the following experiments to test
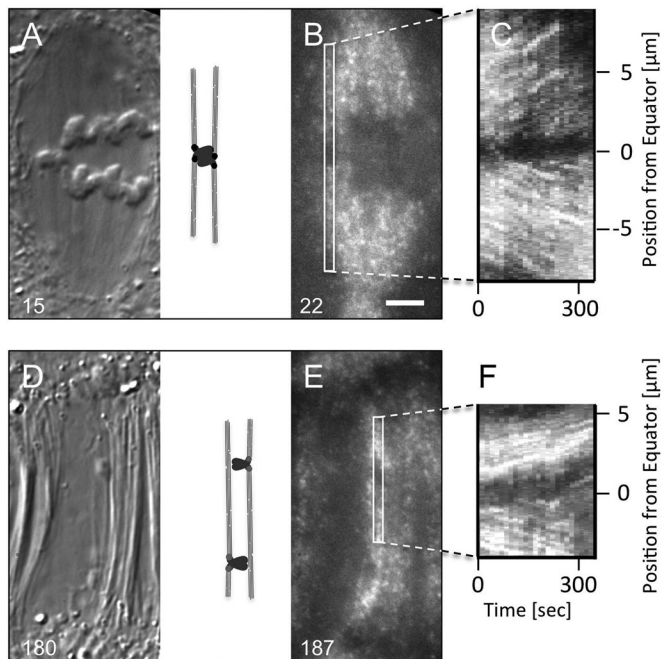
FIGURE 2: (A, B) Pair of DIC (A) and fluorescence (B) images of a spermatocyte in anaphase A after iontophoretic injection of Rh-tubulin. The indicated ROI in (B) locates the area used to generate the kymograph of speckle movements in C. (C) Kymograph record showing speckle tracks in the upper half moving from the univalent toward the upper pole and in the lower half moving from the univalent toward the lower pole. Dark, horizontal region near the center is location of sex chromosome. Supplemental Movie S2, top, contains time-lapse movies of this spermatocyte made by alternating between DIC and fluorescent speckle microscopy modes of imaging. (D, E) Pair of DIC (D) and fluorescence (E) images of a spermatocyte in anaphase B locating the ROI used in generating the kymograph presented in F. (F) Kymograph record showing speckle tracks in upper half moving from leading kinetochore of the univalent toward the upper pole and in the lower half from the trailing kinetochore of the univalent toward the lower pole. Supplemental Movie S2, bottom, is a time-lapse movie of this spermatocyte. A, B, D, E, lower left: time in seconds; bar in B, 5 μm.

the effects of resistive tension as proposed by the model of Maddox *et al.* (2003). We used a laser microbeam to break a univalent's bipolar connection to the two poles and to release one kinetochore from its connection to its sister. If upon release a kinetochore switched to a different functional state, we expected that this would be evident in its postoperation movement.

Release was accomplished by two types of operations using the laser microsurgery tool: 1) Bisection operations separated sisters of a univalent by cutting along the plane of sister chromatid cohesion (Figures 3, A–C, and 4, A–C); the laser flash had the effect of a knife chopping the two sisters apart. 2) Kinetochore ablations knocked out one of the two kinetochore/centromere loci of a univalent (Figures 3, E–G, and 4, E–G). The two complemented each other, in that the former allowed for assessment of both sister kinetochores, whereas the latter facilitated confirmation of detachment of one kinetochore at the expense of the other, especially with LC-PolScope imaging.

Four sets of operations were performed on chromosomes that were stationary laggards at anaphase A or that were engaged in X-Y segregation in anaphase B, as detailed in what follows. In each case, the outcome was initially rapid movement of the released

kinetochores at velocities that exceeded the microtubule flux rate in K-fibers, as observed in control cells described previously.

1. Bisection operations on cells in anaphase A. As presented in Figure 3, C and D, this resulted in immediate anaphase-like movement of both sisters at maximal speeds that averaged ~1.4 μm/min (Table 1), enabling them to quickly catch up to segregating autosomes before the completion of anaphase A (Figure 3D and Supplemental Movie S3, top). After that, their velocities tapered down to a steady-state level of ~0.5 μm/min (based on analysis of slower, steady-state velocity in two cells; Table 1). Bisected sisters were not observed to pass by autosomes.

2. Kinetochore ablations on cells in anaphase A. Ablation of one of the two kinetochores of a univalent at anaphase A (Figure 3, E–H) resulted in the release of the unirradiated sister kinetochore and remaining mass of the univalent from its bipolar attachments (readily apparent with LC-PolScope optics) and its immediate movement toward its pole (Figure 3, E–H, and Supplemental Movie S3, bottom) with average maximal velocities of 1.3 ± 0.3 μm/min (Table 1). Regardless of whether just one kinetochore (of either X or Y) or two kinetochores (one on X and one on Y, either facing the same pole or facing opposite poles) were targeted, the outcome of K ablation was the same: immediate, rapid poleward motion of the unirradiated sister kinetochore, pulling its chromosome arm plus whatever remained of its irradiated sister. Thus, at anaphase A, all four kinetochores of X and Y were capable of poleward movement upon release from their bipolar attachments. Slower steady-state movement after initial rapid release as evident in Figure 3H averaged ~0.7 ± 0.2 μm/min (Table 1).

3. Bisection operations on cells in anaphase B. When bisections were performed to separate sisters during anaphase B (Figure 4, A and B, and Supplemental Movie S4, top)—after X and Y univalents had already developed leading and trailing kinetochores—only the leading kinetochore was capable of further poleward movement, which also was immediate and rapid, moving away from the equator at an average speed of 1.4 ± 0.4 μm/min (Table 1). The trailing kinetochore remained at or near the site of the operation, exhibiting negligible movement to either pole (Figure 4, C and D). Thus, in view of the results obtained from such operations performed during anaphase A—before X-Y segregation had begun—the trailing kinetochore and its K-fiber had lost their capability for poleward motion during the transition from anaphase A to anaphase B. Note that anaphase B operations were performed at times when separation between X and Y was <10 μm, a point when the average rate of X-Y segregation in control cells had not yet reached its peak value.

4. Ablation operations on cells in anaphase B. Targeting of trailing kinetochores, whether on either X or Y, resulted in the same outcome: further, faster movement mediated by the leading kinetochore/kinetochore fiber at average maximal velocities that ranged between 0.9 and 1.7 μm/min (Table 1). The release of an unirradiated leading kinetochore from the drag imposed by its trailing sister was obvious in time-lapse movies (Supplemental Movie S4, bottom, and Figure 4, E–G), in which a leading kinetochore accelerated poleward while pulling the remaining chromosome arms behind. Such responses corroborated the plotted data in Figure 4H, demonstrating that the disconnection of a leading kinetochore from its trailing K-fiber had a recognizable effect on its subsequent movement.
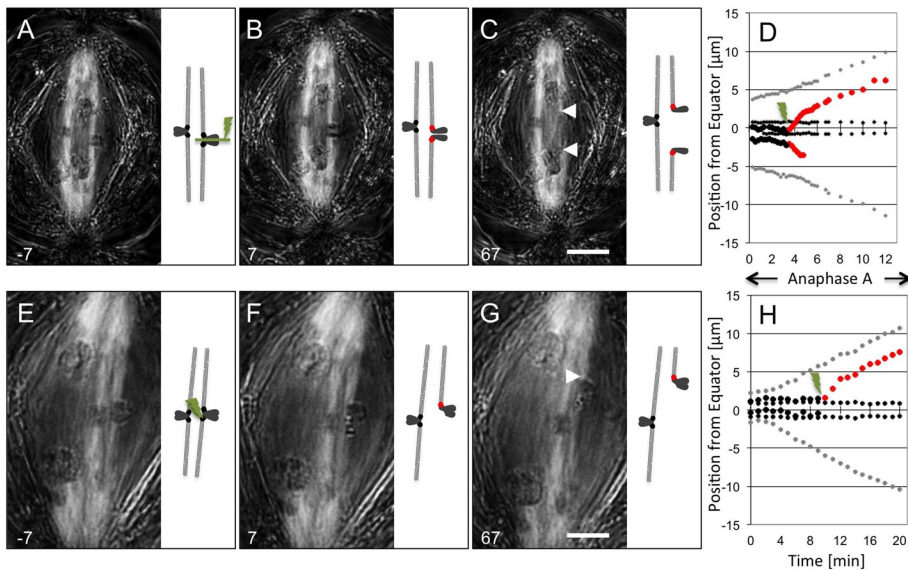
FIGURE 3: Images and schematic drawings of postoperation movement of released kinetochores. (A–C) Anaphase A bisection operation: selected frames from time-lapse imaging with LC-PolScope (Supplemental Movie S3, top). (A) X univalent (on the right) before the laser flash; schematic: laser beam is configured as a line (laser flash: 1-s duration, 5×10^3 pulses, 3 µJ/pulse). (B) First frame after the flash; schematic: released kinetochores in red. (C) At ~1 min after the two sisters are disjoined, they move rapidly toward opposite poles (arrowheads locate kinetochore attachments to birefringent K-fibers); schematic: released kinetochores in red. (D) Plot of positions of poleward edges of kinetochores along the pole-to-pole axis as a function of time: partner autosomes (gray dots) move poleward during anaphase A; before the operation, sister kinetochores of the X univalent (black dots) are positioned at the spindle equator, but subsequent to the flash, separated kinetochores (red dots) lead the way poleward, initially very rapidly but then less so, as they catch up to segregating autosomes. The Y univalent (small black dots) remains as an anaphase laggard during the course of the movie. The released kinetochore moving toward the lower pole disappears from the plane of focus, whereas the progression of its sister poleward was trackable over numerous frames. (E–H) Images and schematics for a point ablation operation of one kinetochore for comparison with the line cut that disjoined sister chromatids in A–C. (E) Target univalent before laser flash; schematic: lightning bolts point to target kinetochore (spot laser flashes: 2×0.5 s in duration, 2×10^3 pulses, 3 µJ/pulse). (F) The released kinetochore (red dot in schematic) moves poleward. (G) The released kinetochore (white arrowhead; red in schematic) leads the way poleward. (H) Distance vs. time plot of positions of poleward edges of kinetochores along the pole-to-pole axis before and after ablation of one kinetochore toward the lower pole. Partner autosomes (gray dots) move poleward during anaphase A. Before the operation, large black dots locate the two sister kinetochores of X at the spindle equator. Subsequent to the flashes, the released kinetochore (red dots) remains connected to and moves to the upper pole, initially very rapidly but then less so, as it catches up to the autosomes. Kinetochores of the Y univalent (small black dots) remain at the equator during the course of the movie (Supplemental Movie S3, bottom). A–C, E–G, lower left: time in seconds referenced to time of laser operation; bar in C, G, 5 µm.

As with anaphase A cells, the initial rapid movement of kinetochores released at anaphase B gradually changed to a slower, steady-state velocity, which we determined to be ~0.6 ± 0.1 µm/min based on postoperation plots from four cells (Table 1).

A direct test shows released kinetochores moving faster than microtubule flux

In view of the flux rates presented in Table 1, the rapid release velocities described here are suggestive of a switch in function of kinetochores and associated microtubule plus ends from polymerization to depolymerization, or reverse pac-man to pac-man motility, with subunit loss at the plus ends of kinetochore microtubules accounting for such fast poleward movement.

For a direct test of this hypothesis, we next performed K ablations on cells that had fluorescently speckled microtubules from preoperation injections. Our objective was to visualize movement of released kinetochores in relation to fluorescent speckles within the associated K-fiber. For this part of the work, we targeted cells in anaphase A because only they provided the postinjection stability that was necessary for this kind of experiment. The reason that anaphase B cells were not useful for these experiments is that intracellular movements as a consequence of X-Y segregation invariably altered our ability to focus on kinetochore targets. This varying target position greatly reduced the possibility of a successful bisection/ablation, and thus the use of anaphase B cells for combined laser microsurgery and fluorescent speckle microscopy was concluded to be impractical with our equipment.

For this experiment, a combination of differential interference contrast (DIC) and fluorescence imaging (see *Materials and Methods*) of rhodamine-tubulin–injected cells was performed to record alternating DIC and fluorescence images that documented the movement of the released kinetochore (DIC images) and the movement of fluorescent speckles in the associated K-fiber (fluorescence images) during anaphase A. A critical step in the subsequent processing and analysis of the two image stacks (e.g., Supplemental Movies S5 and S6) was the marking of the *x-y* pixel location of a released kinetochore obtained from each DIC frame on the subsequent fluorescence mode frame using ImageJ software. With this approach, the poleward movement of such markings in fluorescence movies suggested that 1) kinetochores overtook and then passed by adjacent speckles that were in the kinetochore's poleward path (such speckles must have been within nonkinetochore microtubules of the half-spindle), and 2) kinetochores approached speckles that disappeared as the kinetochore made its way poleward (such speckles are interpreted to have been within the kinetochore's K-fiber and were "gobbled up" by pac-man). In kymographs such as those presented in Figures 5E and 6B, poleward slopes of kinetochores were found to be steeper than slopes of speckles moving poleward in the path taken by the kinetochore to the pole. Kymographs from these experiments also illustrate how poleward velocity of a kinetochore was initially very rapid (faster than flux) and then tapered down to a speed that was similar to that of flux flow. Comparison of speckle flow with such later, slower kinetochore movement in kymographs such as in Figures 5E and 6C revealed both to have average velocity of ~0.7 µm/min. This is interpreted as an indication that the kinetochore is parked on the plus end of its K-fiber, where at those times following the ablation, it engages in neither polymerization nor depolymerization at its kinetochore microtubule plus ends.

Analysis of flux, based on slopes of speckles in kymographs of released kinetochores (including those in Figures 5 and 6), revealed
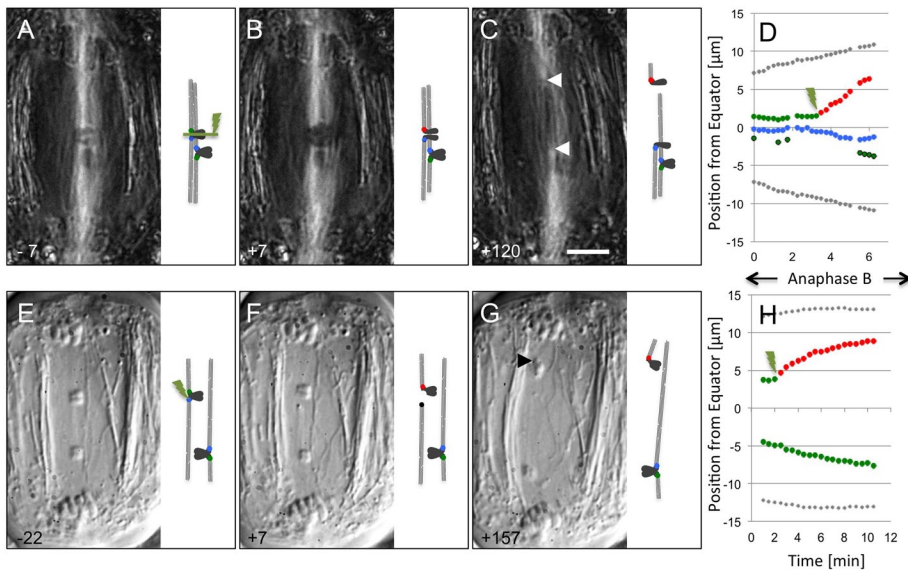
FIGURE 4: (A–C) images and schematics of an anaphase B bisection operation. (A) X univalent before the laser flash; schematic, leading kinetochores are green and trailers are blue; green line indicates the line-shaped laser flash (laser flash: 1-s duration, 5×10^3 pulses, 3 μJ/pulse) made in the interval between A and (B). (B) First frame after the flash; schematic, the leading kinetochore of X (red) begins rapid poleward movement. (C) At ~1 min after the two sisters were disjoined; arrowheads locate the bisected leading (red) and trailing (blue) kinetochores. (D) Plot of positions of poleward edge of a released kinetochore (red) as a function of time: the detached trailing kinetochore (blue dots) remains at or near the equator; the leading kinetochore of Y (lower green dots) continues toward the lower pole; gray dots: edges of autosomes already at the poles; a full chronological sequence for Y was not possible, as it was in an out-of-focus Z-plane for many frames (Supplemental Movie S4, top). (E–H) Selected frames from a DIC time-lapse movie (Supplemental Movie S4, bottom) illustrating X-Y univalents (E) before, (F) just after, and (G) ~4.5 min after the trailing kinetochore of X (upper univalent) was ablated with a spot laser flash. (E) Schematic; lightning bolt points to target kinetochore (laser flash: 5-s duration, 10×10^3 pulses, 3 μJ/pulse). (G) Note the rapid acceleration of its leading kinetochore (arrowhead) poleward immediately after the operation, with the remaining chromatin (lacking its trailing kinetochore) being dragged behind. (H) Plot of positions of poleward edge of the released leading kinetochore of X (red) as a function of time with reference to the spindle equator: gray dots locate edges of autosomes as markers for the spindle poles; the leading kinetochore of Y (green dots) continues poleward, but with a velocity profile much slower than that of the released X. A–C, E-G, lower left: time in seconds referenced to time of laser operation; bar in C, 5 μm.

rates that averaged ~0.7 μm/min. This is in agreement with data from control anaphase A cells as presented in Table 1. Regarding flux after laser ablation, rates in kymographs of K-fibers attached to the motionless (unoperated) partner that remained at the equator in such anaphase A operations also averaged ~0.7 μm/min (Figure 6A). The latter indicates a consistency of flux flow among K-fibers across the breadth of the spindle, and it shows that ablation appeared to have negligible effects on the K-fiber of the released kinetochore.

An additional point is that photobleaching caused by the laser flash eliminated all speckles in the vicinity poleward from the released kinetochore. Thus any comparison of flux rate to kinetochore speed is limited to more poleward, distal speckles. The absence of recovery of fluorescence at the kinetochore end of a K-fiber shows, however, that released kinetochores were without doubt no longer in a polymerization state.

Kinetochores in meiosis II
To address whether laser ablation of one X or Y kinetochore caused collateral damage to its sister, we tracked meiosis II behavior of kinetochores that were released by laser microsurgery performed

during meiosis I. Normally, the behavior of X and Y during meiosis II is the same as that of autosomes: sister kinetochores biorient, they lose cohesion at anaphase onset, and then sisters move to opposite poles as anaphase is completed. Anaphase lagging of X and Y is not normally a feature of meiosis II.

In three of the six cells in which such tracking was done, the formerly unirradiated kinetochore established a kinetochore-to-pole connection with one pole (monotely, confirmed with LC-PolScope), but it did not congress to the spindle equator. During anaphase, the kinetochore-containing portion and the acentric portion shifted to the pole to which the kinetochore was connected. In each of three other cells, the kinetochore established kinetochore-to-pole connections with both poles (merotely, confirmed with LC-PolScope), and it did congress to the equator. During anaphase, the kinetochore and associated arms remained at the spindle equator exhibiting anaphase lag. Eventually during telophase, slight shifting toward one of the poles occurred as the kinetochore fibers appeared to degenerate.

These observed behaviors of released chromosome in meiosis II are similar to observations of others (Khodjakov et al., 1997) made on mitotic chromosome fragments that possessed only one kinetochore. In view of that, we take our meiosis II data as strong evidence that K ablations performed during meiosis I on one of the kinetochores of a univalent did not damage the other, which we observed to be functional during meiosis II.

DISCUSSION
We released X-Y kinetochores from their bipolar connections and from the mechanical resistance that appears to be exerted upon them in such bipolar configurations. Subsequent poleward movement was strikingly faster than normal, at rates twice the flux rate, suggestive that released kinetochores switched from a reverse pacman (polymerization) state to a pac-man (depolymerization) state. Subsequent slower, steady-state rates are consistent with a conversion to a park state in which neither polymerization nor depolymerization occurs.

In search of alternative mechanisms to explain our observations, we considered elastic forces, such as those exerted by chromatin (Larson et al., 2010), and possible contributions of recoil unleashed by the microsurgery. Although we observed short-lived, recoil-type motions in chromosomes and chromosome arms upon release of tension, these movements lasted only for a few seconds and extended over short distances of <1 μm. Furthermore, the release of elastic forces stored inside a chromosome due to opposite pulling forces on its sister kinetochores leads to a shape change of the chromosome that minimally moves its center of mass. In other words, the release of elastic energy stored inside a chromosome does not appreciably move the chromosome's center of mass. It is more plausible that an elastic force that would move the kinetochore and its
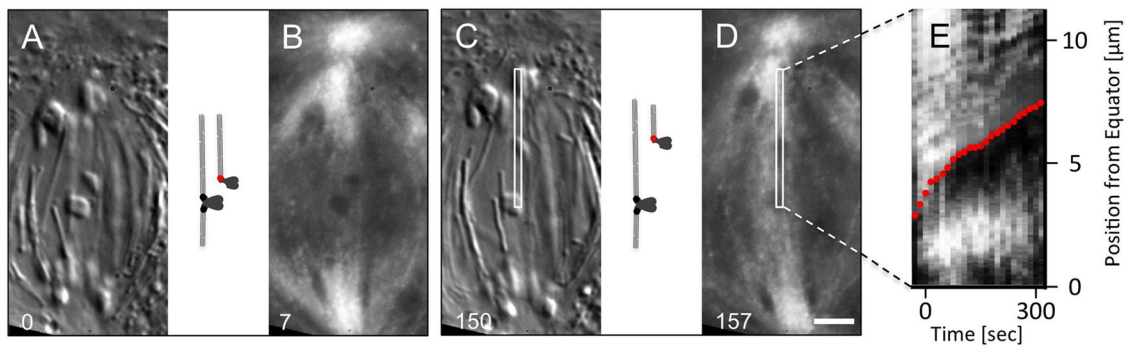
FIGURE 5: (A–D) Selected pairs of DIC and fluorescence images of consecutive frames from a time-lapse sequence showing the chromosome locations and the spindle fluorescence of an injected cell in anaphase A with an ablated single kinetochore of one of the univalents. (E) The contrast-enhanced kymograph made from the ROI indicated in C and D emphasizes the relative movement of the released intact kinetochore (highlighted by red dots) against the fluorescent speckles in its K-fiber. The kymograph analysis and visual inspection of Supplemental Movie S5 reveal the initial velocity of the kinetochore to be almost twice as fast as the speckle flow. Subsequent steady-state velocity of the kinetochore is similar to that of speckles as the released kinetochore moves nearer to the pole. A–D, lower left: time in seconds referenced to time of the start of Supplemental Movie S5; bar in D, 5 μm.

chromosome toward a pole has to come from within the K-fiber. However, our observations are incompatible with an elastic contraction of the K-fiber since speckles inside the fiber moved at the same rate before and after the operation. Furthermore, as microtubules are essentially incompressible along their axis, we are not aware of any molecular mechanism or structure that could exert such elastic forces inside a K-fiber. Also inconsistent with the idea of elastic contraction is our observation during anaphase B operations of the asymmetrical response of the leading and trailing kinetochores. If recoil played a role, one would expect both leading and trailing kinetochores to exhibit poleward movement upon release of tension, which did not occur. Thus our interpretation is that loss of tension unleashed movement because kinetochores switched to a depolymerization state.

Activation of pac-man motility likely entails alterations either in the biochemical makeup of kinetochores or in the activation of mo-

tors that would normally not be activated in this traction fiber system (LaFountain *et al.*, 2001; Wilson *et al.*, 1994). Thus, in crane fly spermatocytes, where heretofore the capability for pac-man motility was not observed, our laser operations appear to have unleashed it. The implications of this are that the molecular machinery for pac-man motility is present in crane fly spermatocytes, but it is not evident when normal mechanical constraints are in operation.

Our experimental results indicate that mechanical tension imposed on segregating X and Y by their bipolar connections is the controlling factor that normally down-regulates pac-man. On severing that connection and relieving the tension, pac-man is activated, and faster-than-flux motility is observed. This interpretation is in accord with the mechanical model proposed by Maddox *et al.* (2003) based on observations made during anaphase in *Xenopus* oocyte extract spindles. Our view is that leading K-fibers represent a traction system, or flux machine, on which leading kinetochores move faster, slower, or at the same speed as flux, depending on the resistance that is imposed on them.

In view of our approach that used speckles within K-fibers as indicators of flux, it is important to recognize that K-fibers in spermatocytes (Scarcello *et al.*, 1986), as in other cells (McDonald *et al.*, 1992), are not uniformly composed of only microtubules that are attached to the kinetochore, but there are also numerous unattached nonkinetochore microtubules that intermingle throughout a K-fiber. Therefore a single speckle observed in our experiments comprises a cluster of fluorophores, some of which are likely attached to kinetochore microtubules and some to nonkinetochore microtubules, but they all are part of the K-fiber that is distinctly recognizable in DIC and fluorescence images. Speckle movements characterized by our experiments represent an average over K-fiber microtubules, and we do not have an understanding of how the dynamic properties of kinetochore versus nonkinetochore microtubules within a given fiber might differ. These are important considerations to be aware of in regard to the interpretation of speckle movements in our experiments.

Findings from our laser experiments have special relevance to the mechanism of X-Y segregation as it occurs in vivo. We propose that pac-man motility normally plays a role in the later stages of X-Y segregation but at stages later than were studied here. In all of the cells included here, the extent of X-Y segregation was 10 μm or less.
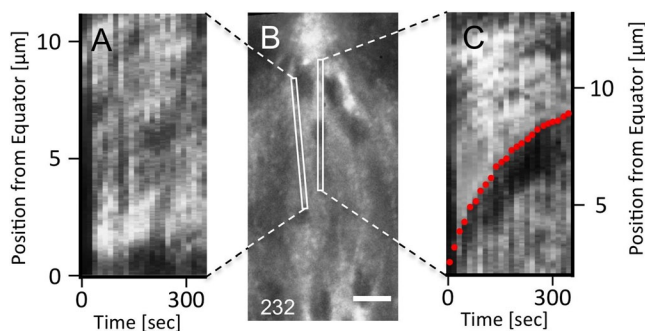
FIGURE 6: (A) Contrast-enhanced kymograph illustrating speckle movement in the K-fiber of the stationary univalent lagging at the equator. (B) A selected fluorescence image from Supplemental Movie S6 taken at time 232 s, which gives the ROIs for generating the kymographs in A and C. (C) Speckle movement in the K-fiber of the released univalent after ablation of one of its kinetochores. Both kymographs have speckle tracks with a slope that is close to the slopes measured in control cells during anaphase A (as shown in Figure 2C and summarized in Table 1). (B) Lower left, time in seconds referenced to time after the start of Supplemental Movie S6; bar, 5 μm.

At such early stages, down-regulation of pac-man would cause segregation rates to be slower than flux rates. Near the end of X-Y segregation, rates of X and Y segregation reach their maxima of ~0.5 µm/min away from the equator (Table 1), which are faster than flux rates of 0.4 µm/min seen at early anaphase B (Table 1). To account for this, our hypothesis is that leading kinetochores are naturally released from trailing resistance at those times and that such release is linked to the eventual disintegration of trailing K-fibers. As alluded to earlier, study of the fate of segregating X-Y K-fibers (both leading and trailing) during anaphase B is hampered by the fact that they become so closely aligned that neither can be distinguished from the other. Nevertheless, it is evident (Supplemental Movie S1) that K-fiber birefringence significantly decreases at the times during anaphase B when segregation rates are maximal (i.e., faster than flux rates). Although the ultimate fate of trailing fibers remains to be determined, this observation serves as a basis for our hypothesis that trailing K-fibers eventually disintegrate in the plane of the former spindle equator. Such a natural release of leading kinetochores from resistive tension offers a ready explanation for the observed shift to faster-than-flux movement during late anaphase B.

Speckles and released kinetochores moved at the same speed after kinetochores started to tail off. We interpret this is as evidence for park—a functional state in which active, motor-based movement does not occur. Our view is that park is another functional state that is down-regulated when a kinetochore is under high tension. It is not clear why pac-man is initially activated and then gives way to park. Nor do we understand the basis for park being a secondary outcome upon sex chromosome release, whereas it appears to be the only outcome upon release of autosomal kinetochores from resistive tension (LaFountain et al., 2011). To speculate, the biochemical composition of autosomal kinetochores and sex univalent kinetochores might be different, or the way resistive forces are leveraged on them may cause different outcomes upon release.

The segregation of X-Y sex univalents is commonly characterized as unorthodox "distance segregation" (Hughes-Schrader, 1969) because X and Y are separated by distance, not physically connected. Yet they segregate to opposite poles during anaphase B. Earlier attempts to understand X-Y segregation focused on the structure of leading and trailing K-fibers (Fuge, 1972, 1985). We propose that there are functional differences between leading and trailing kinetochores at times after X and Y segregation begins, based on two observations. First, as pointed out in Results, as X or Y moves poleward, both leading and trailing kinetochores of each function in a polymerization state. Because the flux rate in leading fibers appears to be the same as that in trailing fibers, poleward movement must be based on subtle differences in the polymerization rates of the leading versus the trailing kinetochore. Specifically, the on rate of the leader must be lower than the on rate of the trailer. In such a scenario, we propose that sex kinetochores would segregate on a "background" of the flux machine, and their movement to opposite poles would be facilitated by a natural imbalance in their polymerization states.

A second observation was that bisection operations showed that the leading kinetochore exhibited capability for further poleward movement, but the trailing kinetochore did not. The trailer remained essentially motionless, not moving toward either pole. When bisections were performed before X-Y segregation had begun, both sisters of either univalent exhibited poleward movement. These results demonstrated that each univalent has a "trailing kinetochore in waiting" that makes a switch in functional state to "neutral" (Skibbens et al., 1993; Khodjakov and Rieder, 1996). By definition, a neutral kinetochore lacks capability for poleward motility but can facilitate

elongation of its K-fiber in response to forces exerted to the opposite pole. Neutral then is another type of polymerization state evident in kinetochores moving away from the pole to which they are attached. Based on their behavior after bisections, detached trailing kinetochores appear to have retained their polymerization capabilities, in view of their lack of movement to either pole. However, the polymerization function of detached trailers was not tested, and thus this remains open to investigation.

Regarding the mechanism by which a univalent kinetochore is "tagged" for undergoing conversion to neutral, this is a question within the larger, long-standing question of how distance segregation in general is achieved. Sillers and Forer (1981) suggested that the switch for initiating the segregation of X and Y to opposite poles entailed turning on motors associated with leading K-fibers, whereas trailing-fiber motors remained turned off. The present data suggest that the capability for poleward motion of all sex kinetochores (on both X and Y) exists before segregation occurs. Hence the conversion of trailing kinetochores to neutral more likely is the switch that must be tripped in order to convert one kinetochore per univalent to neutral, thus facilitating segregation of X from Y. To bring about such conversions, there may be a number of biochemical alterations that must be made either through addition and/or removal of specific kinetochore protein components or through phosphorylation/dephosphorylation of constitutive kinetochore proteins.

In conclusion, we provided a new piece to an existing body of evidence that continues to mount for the concept that kinetochore function is subject to regulation by tension. Recent advances made in vitro (Akiyoshi et al., 2010) exemplify how research on the influence of tension on interactions between kinetochores and microtubules is moving to the molecular level. Challenges for the future will be to understand the molecular mechanisms by which kinetochore proteins bring about switches in kinetochore motility such as those observed here.

MATERIALS AND METHODS

Spermatocytes from fourth-instar crane fly (N. suturalis) larvae were cultured under oil (Voltalef 10s oil; Atofina, Puteaux, France) at the oil–glass interface of a coverglass that was either mounted to a glass slide (LaFountain and Oldenbourg, 2004) or part of a well-slide preparation (Janicke and LaFountain, l986). Cells cultured in this way survive for hours, permitting observation of both meiotic divisions from start to finish. In spermatocytes, diploid is eight: three pairs of metacentric autosomes and a pair of telocentric sex chromosomes X and Y. Y is slightly smaller than X.

For laser microsurgery, a nanosecond-pulsed solid-state laser (laser head SNG-03E-TB1, Teem Photonics [Meylan, France]; wavelength, 532 nm; pulse energy, 3 µJ; pulse duration, 1 ns; repetition rate, up to 10 kHz) was directed to the specimen through the epi-port of an inverted microscope (Axiovert 200M [Zeiss, Jena, Germany] or Diaphot 300 [Nikon, Melville, NY]). The design of the laser optical pathway and the triggering of laser pulses were detailed in an earlier report (LaFountain et al., 2011). The shape of the laser beam in the specimen plane was chosen to be either a spot or a line. For spot ablation, the suitably expanded beam was focused into the conjugate image plane near the epi-port using a plan-convex doublet with 25-mm focal length. For line ablation, an additional cylindrical lens (focal length 150 mm) was placed ~150 mm before the doublet lens so as to expand the focal spot in one direction. A laser flash of 0.5–1.0 s in duration, with the signal generator operating at 2–5 kHz, was sufficient to achieve the intended cutting or ablation operation.

For experiments that investigated microtubule flux after laser microsurgery, a suitable cell was identified using DIC imaging, and then microinjection of rhodamine-conjugated tubulin (Cytoskeleton, Denver, CO) was done using a previously described iontophoretic approach (LaFountain et al., 2004). Observation of postinjected cells continued using DIC and long-wavelength light that did not excite or bleach the fluorophore. While imaging the cell, the kinetochore best suited for the operation was positioned at the optical path of the laser beam by manual adjustment of the stage. The operation was performed by the laser beam (attenuated to 10% of full power) as soon as anaphase began. Imaging subsequent to the laser flash was done using a combination of DIC and fluorescence optics with time-lapse intervals between frames that were usually 7.5 s, resulting in the combined DIC/fluorescence series having 15-s intervals for the DIC portion and 15-s intervals for the fluorescence portion. To maintain registration between DIC and fluorescence images, we used the same imaging optics, including the same camera, for recording both types of images. To prevent potential image shift between DIC and fluorescence images, we kept the fluorescence cube in the imaging path when recording DIC images. The wavelength of the transmitted illumination for DIC was within the passband of the fluorescence emission filter.

Acquisition of fluorescence images immediately before or during laser operations was not possible with our microinjection/laser microsurgery/image acquisition rig. This limitation was because the intended ablation was performed in DIC mode, and success of the operation had to be confirmed by continued observation before starting the imaging regimen. Then, after such confirmation, a movie was made in time lapse by alternating between fluorescence and DIC modes over the course of 6 min, after which fluorescence diminution of the entire spindle made further imaging impractical. With this approach, the first minute or so of a released kinetochore's movement, as well as similar segment of FSM, was not recorded. Evident in supplemental movies is the result that each laser flash resulted in immediate photobleaching around the flash site (LaFountain et al., 2011), an outcome that eliminated all speckles that were adjacent to kinetochores before the flash. Nevertheless, sufficient speckles in regions distal to kinetochores remained to make speckle analysis possible.

For a given ablation experiment, we collected DIC and fluorescence images into separate stacks and analyzed kinetochore movements and microtubule flux by preparing kymographs using both image types. Before creating a kymograph, however, we registered consecutive frames of a time-lapse series to counteract any global drift of the cell under observation. The registration included the following steps: the K-fiber in question was first oriented vertically and then translated to bring the K-fiber to the same lateral position. The vertical registration was referenced to the spindle equator, which was moved to the same vertical position in each frame. To achieve this type of registration, consecutive frames of DIC images were rotated and shifted as needed, identifying the K-fiber in question by its weak but distinct DIC contrast, and identifying the equator as the half-distance between spindle poles and/or half-point between the chromosomal mass of the segregated autosomes. For registering the equator in images taken during anaphase A, we used the intact univalent that remained at the equator as a laggard as a reference point. For each DIC image the needed rotation and translation was noted and then repeated for its fluorescence counterpart so as to maintain equal registration between DIC and fluorescence images.

For creating kymographs we used image-processing functions available in IP Lab and ImageJ (National Institutes of Health,

Bethesda, MD). With IP Lab, we used a customized PROJECTION script that incorporated a number of IP Lab commands, including the 3D Projector command to create a projection stack in which the movement of fluorescent speckles from one frame to the next was displayed as a function of time within the resultant three-dimensional projection. With ImageJ, we used similar projection algorithms available as menu items called Reslice… and Z-Project. Projections are similar to kymographs used to display time-dependent speckle movement as reported by others (Waterman-Storer et al., 1998). Included in the steps of making a kymograph is establishment of a region of interest (ROI), the contents of which are then converted by the algorithm into a kymograph. For example, consider the ROIs in Figure 5, C and D, which define the portions of those images that were used for kymographs. In these cases, the ROI is positioned over the K-fiber imaged in the DIC image (Figure 5C) and fluorescence image (Figure 5D), and thus we assume that speckles within the ROI in the fluorescence image move within the K-fiber.

For analysis of kinetochore separation rates, the poleward edges of leading kinetochores as they appeared in DIC or phase contrast images were referenced and their separation distance was measured using ImageJ tools as a function of time. With LC-PolScope images (Oldenbourg and Mei, 1995), the sites of connection between kinetochores and their birefringent kinetochore fibers were reference points. For analysis of velocities of released kinetochores, the spindle equator was the reference; its location was determined based on the position of the polar basal bodies (or another suitable structure, if the basal bodies were not in focus). Data were imported into Excel software (Microsoft, Redmond, WA) for plotting.

For some experiments with anaphase B cells, pretreatment of testes before rupturing them under oil was done for 5 min in a buffer solution containing 2 μm cytochalasin D (CD) to inhibit cytokinesis and thereby prevent any influence that in-furrowing at the cell periphery might have on chromosome behavior in the cell interior. This also prevented the incursion of mitochondria into the interzone during anaphase B, so that domain of the spindle remained optically clear for optimal tracking of both anaphase B chromosomes and their kinetochore fibers. The effect of such low-dose CD pretreatment was cytokinesis specific, as expected based on earlier work (LaFountain et al., 1992), and no difference was evident upon comparing results obtained with pretreated cells with those from untreated controls.

REFERENCES
Akiyoshi B, Saragapani KK, Powers AF, Nelson CR, Reichow SL, Arellano-Santoyo H, Gonen T, Ranish JA, Asbury CL, Biggins S (2010). Tension directly stabilizes reconstituted kinetochore-microtubule attachments. Nature 468, 576–579.

Begg DA, Ellis GW (1979a). Micromanipulation studies of chromosome movement. I. Chromosome-spindle attachment and the mechanical properties of chromosomal spindle fibers. J Cell Biol 82, 528–541.

Begg DA, Ellis GW (1979b). Micromanipulation studies of chromosome movement. II. Birefringent chromosomal fibers and the mechanical attachment of chromosomes to the spindle. J Cell Biol 82, 542–554.

Fuge H (1972). Morphological studies on the structure of univalent sex chromosomes during anaphase movement in spermatocytes of the crane fly Pales ferruginea. Chromosoma 39, 403–417.

Fuge H (1985). The three-dimensional architecture of chromosomal fibers in the crane fly. II. Amphitelic sex univalents in meiotic anaphase I. Chromosoma 91, 322–328.

Hughes-Schrader S (1969). Distance segregation and compound sex chromosomes in Mantispids (Neuroptera; mantispidae). Chromosoma 27, 109–129.

Janicke MA, LaFountain JR Jr (1986). Bivalent orientation and behavior in crane-fly spermatocytes recovering from cold exposure. Cell Motil Cytoskeleton 6, 492–501.

Khodjakov A, Cole RW, McEwen BF, Buttle KF, Rieder CL (1997). Chromosome fragments possessing only one kinetochore can congress to the spindle equator. J Cell Biol 136, 229–240.

Khodjakov A, Rieder CL (1996). Kinetochores moving away from their pole do not exert a significant pushing force on the chromosome. J Cell Biol 135, 315–327.

LaFountain JR Jr, Cohan CS, Oldenbourg R (2011). Functional states of kinetochores revealed by laser microsurgery and fluorescent speckle microscopy. Mol Biol Cell 22, 4801–4808.

LaFountain JR Jr, Cohan CS, Siegel AS, LaFountain DJ (2004). Direct visualization of microtubule flux during metaphase and anaphase in crane-fly spermatocytes. Mol Biol Cell 15, 5724–5732.

LaFountain JR Jr, Cole RW, Rieder CL (2002). Partner telomeres during anaphase in crane-fly spermatocytes are connected by an elastic tether that exerts a backward force and resists poleward motion. J Cell Sci 115, 1541–1549.

LaFountain JR Jr, Janicke MA, Balczon R, Rickards GK (1992). Cytochalasin induces abnormal anaphase in crane-fly spermatocytes and causes altered distribution of actin and centromeric antigens. Chromosoma 101, 425–441.

LaFountain JR Jr, Oldenbourg R (2004). Maloriented bivalents have metaphase positions at the spindle equator with more kinetochore microtubules to one pole than to the other. Mol Biol Cell 15, 5346–5355.

LaFountain JR Jr, Oldenbourg R, Cole RW, Rieder CL (2001). Microtubule flux mediates poleward motion of acentric chromosome fragments during meiosis in insect spermatocytes. Mol Biol Cell 12, 4054–4065.

Larson ME, Harrison BD, Bloom K (2010). Uncovering chromatin's contribution to the mitotic spindle: applications of computational and polymer models. Biochemie 92, 1741–1748.

Maddox P, Straight A, Coughlin P, Mitchison TJ, Salmon ED (2003). Direct observation of microtubule dynamics at kinetochores in *Xenopus* extract spindles: implications for spindle mechanics. J Cell Biol 162, 377–382.

McDonald KL, O'Toole ET, Mastronarde DN, McIntosh JR (1992). Kinetochore microtubules in PTK cells. J Cell Biol 118, 569–383.

Mitchison TJ (2005). Mechanism and function of poleward flux in *Xenopus* extract meiotic spindles. Philos Trans R Soc Lond B Biol Sci 360, 623–629.

Nicklas RB (1997). How cells get the right chromosomes. Science 275, 632–637.

Nicklas RB, Koch CA (1969). Chromosome micromanipulation. III. Spindle fiber tension and the reorientation of mal-oriented chromosomes. J Cell Biol 43, 40–50.

Nicklas RB, Ward SC (1994). Elements of error correction in mitosis: microtubule capture, release and tension. J Cell Biol 126, 1241–1253.

Oldenbourg R, Mei G (1995). New polarized light microscope with precision universal compensator. J Microsc 180, 140–147.

Rogers GC, Rogers SL, Sharp DJ (2005). Spindle microtubules in flux. J Cell Sci 118, 1105–1116.

Scarcello LA, Janicke MA, LaFountain JR Jr (1986). Kinetochore microtubules in crane-fly spermatocytes: untreated, 2°C-treated, and 6°C-grown spindles. Cell Motil Cytoskeleton 6, 428–438.

Sillers PJ, Forer A (1981). Autosomal spindle fibres influence subsequent sex-chromosome movements in crane-fly spermatocytes. J Cell Sci 49, 51–67.

Skibbens RV, Skeen RP, Salmon ED (1993). Directional instability of kinetochore motility during chromosome congression and segregation in mitotic newt ling cells: A push-pull mechanism. J Cell Bio 859–875.

Waterman-Storer CM, Desai A, Bulinski JC, Salmon ED (1998). Fluorescent speckle microscopy, a method to visualize the dynamics of protein assemblies in living cells. Curr Bio 8, 1227–1230.

Waters JC, Mitchison TJ, Rieder CL, Salmon ED (1996). The kinetochore microtubule minus-end disassembly associated with poleward flux produces a force that can do work. Mol Biol Cell 7, 1547–1558.

Wilson PJ, Forer A, Leggiadro C (1994). Evidence that kinetochore microtubules in crane-fly spermatocutes disassemble during anaphase primarily at the poleward end. J Cell Sci 107, 3015–3027.